



Article

The Impact of Storm-Induced Breaches on Barrier Coast Systems Subject to Climate Change—A Stochastic Modelling Study

Koen R. G. Reef ^{1,*} , Pieter C. Roos ¹, Tessa E. Andringa ¹ and Ali Dastgheib ²
and Suzanne J. M. H. Hulscher ¹ 

¹ Water Engineering and Management, University of Twente, 7522 NB Enschede, The Netherlands; p.c.roos@utwente.nl (P.C.R.); tessa_andringa@hotmail.com (T.E.A.); s.j.m.h.hulscher@utwente.nl (S.J.M.H.H.)

² Department of Water Science and Engineering, IHE Delft Institute for Water Education, P.O. Box 3015, 2601 DA Delft, The Netherlands; a.dastgheib@un-ihe.org

* Correspondence: k.r.g.reef@utwente.nl

Received: 14 March 2020; Accepted: 3 April 2020; Published: 10 April 2020



Abstract: Storms can have devastating impacts on barrier coasts causing coastal erosion, partial inundation, and possibly the breaching of barrier islands. The breaching of barrier islands provides a mechanism for the creation of new tidal inlets that connect the backbarrier basin (or lagoon) and the outer sea. As a new tidal inlet affects both the basin and the hydrodynamics of existing inlets, it is important to understand why an initial breach either closes or may evolve into a new tidal inlet. To this end, we performed a Monte Carlo analysis using an idealized model capable of simulating the long-term morphological evolution of multiple tidal inlets connected to a single backbarrier basin. To do so required the creation of a stochastic shell, as a new element around this existing barrier coast model. Our results demonstrate that barrier coast systems tend towards an equilibrium value for the number of inlets per kilometer of barrier coast and total inlet cross section. This even holds with the continuous stochastic forcing of storm-induced breaches. This finding implies that if a new breach opens in a coast that is already in equilibrium, existing inlets will shrink and may close if the new breach remains open. Furthermore, we find that climate-driven changes in storm frequency will modify the timescales in which barrier coasts reach their equilibrium state. Finally, we find that the distance between a new breach and its nearest neighbor is more important for its survival than the size of the breach or the degree of saturation of the barrier coast.

Keywords: barrier island breaching; multi-inlet systems; morphodynamic modelling; meso-tidal barrier coasts; monte carlo simulation; idealized modelling

1. Introduction

Barrier coasts are important dynamic systems that cover around 10% of the coastlines worldwide [1,2]. Due to their ecologic, economic, and touristic worth, they are often densely populated [3,4]. Barrier coasts are highly dynamic systems whose morphology continuously changes under the influence of tides, waves, and storms [5]. The large-scale morphology of barrier coast systems is controlled by the relative importance of tides and waves [6]. This study focusses on meso-tidal barrier coasts, that is those in which tides and (fair-weather wind) waves are of equal importance.

A key aspect of the natural morphological evolution of barrier coast systems is the evolution of the tidal inlets, which form the connection that links the outer sea to the inner tidal basin. The impact of tides and waves on the evolution of a single tidal inlet system has already been studied by Escoffier [7] who showed that for an inlet to be in a morphological equilibrium, the sediment export due to the

tide should be balanced by the wave-induced sediment import into the inlet. This equilibrium for multiple-inlet systems is also influenced by the interaction between various elements, such as between the inlets themselves and between the inlets and the backbarrier basin.

Evidence for this interaction comes from the observed residual circulation in backbarrier basins [8–10], the role of spatially varying backbarrier basin hydrodynamics in the stability of multiple tidal inlets [11,12], and the fact that the total tidal prism entering a backbarrier basin is primarily a system characteristic that is barely affected by the configuration of the tidal inlets [13].

Storms also significantly affect barrier coasts despite the fact that they are less frequent and more episodic than tides and waves. The effects of storms on barrier coasts range from coastal erosion and local inundation to the breaching of barrier islands [14,15]. This breaching of barrier islands is one of the mechanisms through which new tidal inlets may form. Regions that commonly experience storm-induced breaches include the east coast of the United States of America (USA) [16,17] and the Ria Formosa in Portugal [18,19]. These breaches can have a lasting impact on the entire barrier coast system, as a new inlet conveys a part of the total tidal prism entering the backbarrier basin, and alters tidal dynamics [20,21].

Examples of the breaching of barrier islands are plentiful. During Hurricane Sandy in 2012 the barrier chain south of Long Island (NY, USA) was breached at three locations, two of them at Fire Island and one at Westhampton [22]. However, at the beginning of 2020, only one of those breaches in Fire Island was still open, now called Old Inlet, whereas the other two breaches were closed artificially (see Figure 1). Another example is the Core Sound, the southern part of the North Carolina (USA) outer banks, where three inlets—Old Drum, New Drum, and Ophelia Inlet—have alternately opened and closed under the influence of storm-induced breaches (see Figure 2).

These examples illustrate that storm-induced breaches have a profound effect on nearby inlets and the tidal dynamics in the backbarrier basin. However, this effect is still poorly understood. Therefore, the goal of this study is to investigate the impact of storm-induced breaches on inlets connected to the same backbarrier basin and on the interaction among these inlets. Specifically, we aim to answer the following research questions:

- How do storm-induced breaches affect existing inlets connecting to the same backbarrier basin and what are the interactions between them?
- What breach characteristics determine whether a breach evolves into an open inlet or closes?
- How are multiple-inlet systems affected by climate driven changes in the storm climate?

To answer our research questions, we need to overcome a methodical challenge as no standard approach exists to combine the two types of driving forces that we consider—storms, occurring on an irregular basis, and tides and waves that continuously affect barrier coast systems [4]. Our approach is to extend an existing idealized barrier coast model that simulates the morphological evolution of tidal inlets under the influence of tides and waves [12] by adding a stochastic shell around the model. This innovation allows the stochastic forcing of storm-induced breaches by determining whether or not breaches at each moment in the morphological evolution. We select an idealized barrier coast model as it allows us to study the effect of individual processes and its low computational cost allows us to systematically study the breach characteristics that determine whether a storm-induced breach remains open or not.

This work is organized as follows. First, the methods including the development of our stochastic shell are presented in Section 2, followed by the results in Section 3, the discussion in Section 4, and finally the conclusions in Section 5.



Figure 1. Satellite images of three storm-induced breaches at Fire Island and Westhampton (Long Island, NY, USA) due to hurricane Sandy in 2012 showing: (a) before the storm (7 March 2012); (b) shortly after the storm (4 November 2012); (c) almost one year after the storm (20 September 2013). The location of the breaches is indicated with yellow circles. Retrieved from Google Earth (Map Data: DigitalGlobe, USDA Farm Service Agency).

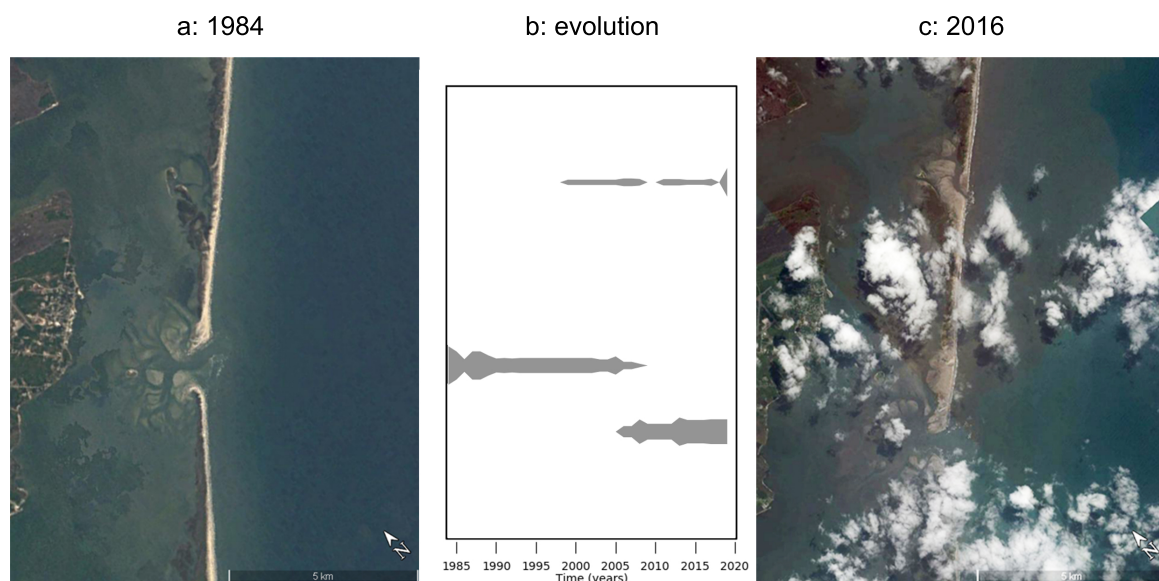


Figure 2. Evolution of three tidal inlets—Old Drum (top), New Drum (middle), and Ophelia Inlet (bottom)—that have alternately opened and closed at Core Sound, NC, USA. Shown are satellite images from 1984 (panel a) and 2016 (panel c), as well as the evolution (panel b) based on satellite image analysis. After the closing of Old Drum Inlet, New Drum Inlet was opened artificially in 1971. At the site of Old Drum Inlet, (New) Old Drum Inlet opened in 1999 as a storm-induced breach during Hurricane Dennis, and in 2005 Hurricane Ophelia opened Ophelia Inlet south of New Drum Inlet [23]. Later, both Old and New Drum Inlet closed, but were reopened by Hurricane Irene in 2011. At the start of 2020 both Ophelia and Old Drum Inlet are open and New Drum inlet has closed. Data from Satellite images from Google Earth (Map Data: Landsat/Copernicus).

2. Methods

Previous studies on the long-term evolution of (multiple) inlet systems have used simulation models as long-term measurements are not available for a wide range of barrier coasts. Examples of models that have been used include semi-empirical models (e.g., ASMITA [24]), complex process-based models (e.g., Delft3D [25]), and idealized models (e.g., Reference [12]). However, none of these models have been combined with a stochastic forcing of storm-induced breaches. This can be partially attributed to the absence of a standard approach to combine stochastic forcing (storms) and deterministic forcing (tides and waves) in barrier coast modelling [4].

We build a stochastic shell around an existing idealized barrier coast model [12] to allow us to stochastically force storm-induced breaches. This model is outlined in Section 2.1, the stochastic shell is presented in Section 2.2, and the design of our model experiments in Section 2.3.

2.1. Idealized Barrier Coast Model

The idealized barrier coast model developed by Roos et al. [12] and described in Reef et al. [13] will be used in this study to simulate the morphological evolution of multiple tidal inlets as it combines the impact of tides and waves on the morphological evolution of inlets. The model domain is represented by a simplified geometry consisting of multiple tidal inlets that connect a rectangular inner tidal basin having a spatially uniform depth to the outer sea where the system is forced by a tidal wave. The j tidal inlets have a length l_j , a cross-section A_j , and constant shape defined by a shape factor $\gamma^2 = h_j/b_j$ (e.g., Reference [5]). The rectangular tidal basin is characterized by a longshore length L , cross-shore width B , and depth h_b . Finally, on the semi-infinite outer sea of depth h_o , a tidal wave is forced with amplitude Z and tidal frequency ω .

The model consists of a hydrodynamic and a morphodynamic part. The morphodynamic part is based on the stability concept of Escoffier [7] and combines a constant sediment import M with a sediment export X_j that is based on the velocity amplitude of the tide in an inlet. The balance of these sediment fluxes determines dA_j/dt , that is an inlet accretes ($M > X_j$), erodes ($M < X_j$), or is in equilibrium ($M = X_j$).

The hydrodynamic part is based on the linearized shallow water equations with linearized bottom friction in the basin and inlet channels according to Lorentz' linearization, and it simulates the hydrodynamics in the entire domain. It is forced by a tidal wave on the outer sea with amplitude Z and tidal frequency ω . The morphodynamic part of the model is solved numerically using a forward Euler discretization (with timestep Δt), while the hydrodynamic part is analytically reduced to a linear system of equations that are solved using standard techniques.

In their simulations, Roos et al. [12] started with an oversaturated barrier coasts (i.e., with far more inlets than the equilibrium configuration) and simulate the morphological evolution of the tidal inlets over centuries towards an equilibrium (or near-equilibrium) configuration in which some inlets remained open and some have closed. They found that their model results agree with observed relationships between inlet characteristics and both tidal range and tidal basin width.

2.2. Stochastic Shell: Forcing Storm-Induced Breaches

To stochastically force storm-induced breaches in the model of Roos et al. [12], we develop a stochastic shell around this model. At every timestep, this shell determines whether or not storm-induced breaches are created—and, if so, what their properties are—see Figure 3. This is done in three steps:

- Step 1 determines the number of storms n_s that occur during the timestep,
- Step 2 determines the number of breaches n_b that occur (if $n_s > 0$),
- Step 3 determines the initial inlet cross-section A_{init} and inlet location y_j of each newly created breach (if $n_b > 0$).

In these three steps, we use three different Probability Density Functions (PDFs). In step one, to determine the number of storms n_s that occur during a timestep we use a Poisson distribution as it shows the best fit with the Annual Hurricane Occurrence dataset [26], that is,

$$p(n_s) = \frac{\lambda_s^{n_s}}{n_s!} e^{-\lambda_s}. \quad (1)$$

Here we use a mean value λ_s that is the inverse of the location specific recurrence times for hurricanes as determined by Keim et al. [27].

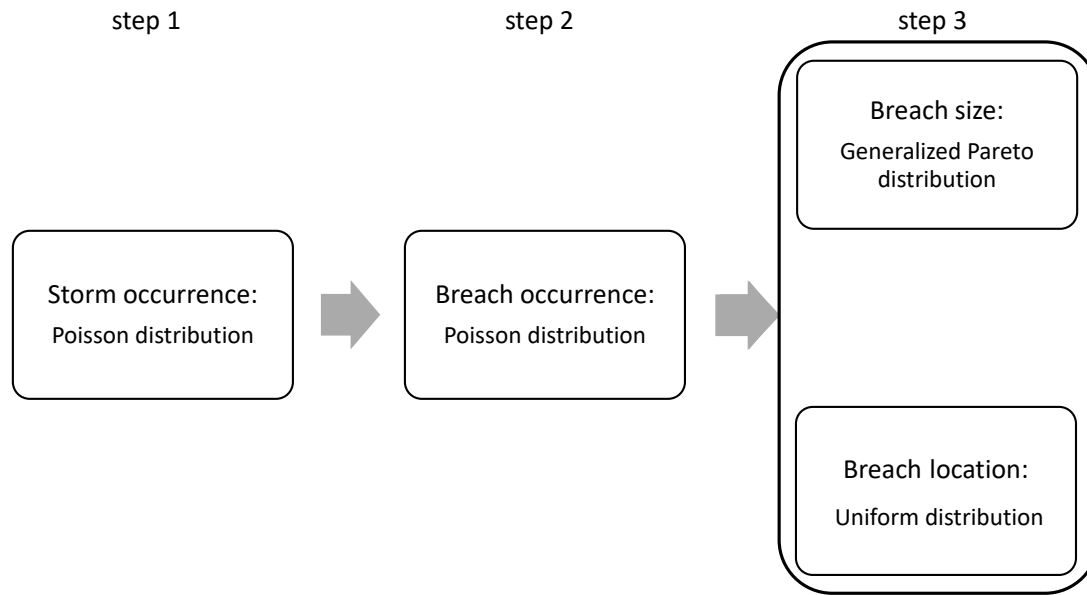


Figure 3. Diagram showing the procedure used in our stochastic shell to determine if storm-induced breaches are forced and what their characteristics will be. Further explanation in Section 2.2.

Because only little data is available on storm-induced breaches, and particularly about their occurrence, we assume that the occurrence and initial size can be modelled using the same PDFs as the occurrence and intensity of storms. Therefore, we also use a Poisson distribution in step two to determine the number of breaches n_b per storm, that is,

$$p(n_b) = \frac{\lambda_b^{n_b}}{n_b!} e^{-\lambda_b}. \quad (2)$$

Here we assume a mean value $\lambda_b = 1$ per storm due to a lack of data on the number of breaches per storm.

In step three, we use a Generalized Pareto distribution to determine the initial inlet cross-section A_{init} as it was found to be the best for the intensity of storms in the Annual Hurricane Occurrence dataset [26]

$$p(A_{\text{init}}) = \left(\frac{1}{\sigma}\right) \left(1 + k \frac{(A_{\text{init}} - \theta)}{\sigma}\right)^{(-1-\frac{1}{k})}. \quad (3)$$

Here the scale $\sigma = 243 \text{ m}^2$, shape $k = 7.84 \times 10^{-9}$, and location $\theta = 38 \text{ m}^2$ were fitted using data from 19 historic breaches [22,23,28–36].

Finally, also in the third step, we use a uniform distribution to determine the inlet location y_j because we assume that the likelihood of a breach is considered the same for every part of the barrier coast (except for existing inlets). This implies

$$p(y_j) = \begin{cases} 0 & \text{for } y_j \text{ at an inlet,} \\ \frac{1}{L_{\text{res}}} & \text{for } y_j \text{ not at an inlet.} \end{cases} \quad (4)$$

Here $L_{\text{res}} = L - \sum_{j=1}^J b_j$ is the length of the barrier coast minus the cumulative width of all open inlets.

2.3. Design of Model Experiments

2.3.1. Outline of a Single Simulation

We start each simulation with a barrier coast without any inlets at $t = 0$ and subsequently force a storm event that induces at least one storm-induced breach. To do so, we start at step two in our stochastic shell and keep repeating this procedure until at least one (possibly more) storm-induced breach is created. This starting procedure is different from Roos et al. [12] where each simulation was initialized with an oversaturated barrier coast (i.e., with more inlets than in equilibrium). Next, the model simulates the evolution of the storm-induced breaches toward a final inlet configuration over a period of 1000 years.

At every timestep, two morphological changes are considered. First, the stochastic shell determines whether or not storm-induced breaches are generated (see Section 2.2). Second, similar to References [12,13] we simulate the morphological evolution of the tidal inlets based on the stability concept of Escoffier [7] (see Section 2.1).

The resulting final inlet configurations are analyzed using three metrics: the ratio of equilibrium inlet cross-section and the mean initial size $A_{j,\text{all}}/A_\mu$ (-), the number of open inlets per km barrier coast J_{total}/L (km^{-1}), and the relative total tidal prism $P_{\text{total}}/P_{\text{ref,total}}$ (-) with

$$P_{\text{total}} = \sum_{j=1}^J \frac{2|\hat{u}_j|}{\omega} A_j \quad \text{and} \quad P_{\text{ref,total}} = Z A_{\text{basin}} = ZBL. \quad (5)$$

Here, the tidal prism for a single inlet (i.e., $\frac{2|\hat{u}_j|}{\omega} A_j$) is obtained by integrating the sinusoidal tidal velocity signal $|\hat{u}_j|$ in an inlet over half a tidal cycle and multiplying the result by the inlet cross-section A_j .

Two sets of parameter values are used in this work. The first represents the Great South Bay system (NY, USA) and the second the Core Sound system (NC, USA), both can be found in Table 1.

Table 1. Model parameters used in this study.

Parameter	Symbol (unit)	Great South Bay	Core Sound
Tidal Elevation Amplitude in sea	Z (m)	0.5	0.325
Tidal Frequency in sea	ω (rad/s)	1.405×10^{-4}	1.405×10^{-4}
Basin Depth	h_b (m)	1.3	2
Basin Length	L (km)	40	30
Basin Width	B (km)	5	5
Drag Coefficient	c_d (-)	2.5×10^{-3}	2.5×10^{-3}
Inlet Length	l_j (km)	0.5	1
Mean Initial Inlet Cross Section	A_μ (m^2)	281	281
Inlet Shape Factor	γ^2 (-)	0.005	0.005
Outer Sea Depth	h_o (m)	10	10
Sediment Import	M (m^3/year)	4×10^5	8.25×10^5
Mean number of Hurricanes per year	λ_s (year^{-1})	1/35	1/5
Morphodynamic Timestep	Δt (year)	0.5	0.5
# of Simulations in one Ensemble	n (-)	500	500

2.3.2. Monte Carlo Simulation

To systematically analyze the effect of storm-induced breaches we perform two Monte Carlo ensembles simulation consisting of $n = 500$ individual simulations, for both the Great South Bay and Core Sound sets of parameter values (see Table 1). In every simulation different storm-induced breaches are forced, therefore we expect different final configurations for every simulation as well. To aggregate these results, we determine the median and 50% envelope over all simulations in the ensemble using the same metrics as above.

We also use these results to investigate which breach characteristics determine whether or not a storm-induced breach remains open. This is done by analyzing the effect of three breach characteristics:

- the relative size of the breach A_{init}/A_{μ} ,
- the barrier coast saturation J/J_{μ} ,
- the distance of a breach to the nearest neighboring inlet d_{nearest} .

To do so, we compute 2D histograms showing the breach survival rate of all three combinations of taking two of the three breach characteristics. The chance of breach survival over the entire simulation is defined as

$$p_{\text{survival}} = \frac{N_{\text{open}}}{N_{\text{open}} + N_{\text{closed}}}, \quad (6)$$

where N_{open} is the total number of breaches that remained open and N_{closed} is the total number of breaches that closed, both determined per histogram bin.

To study the effect of changes in storm climate we vary the storm frequency λ_s in the stochastic shell from -50% to $+50\%$ in 11 Monte Carlo ensemble simulations, consisting of 500 individual simulations each. The range of change in storm frequency from -50% to $+50\%$ is the span of the 67% confidence interval for tropical storm frequency (with a median just under 0), by the IPCC [37]. These results are analyzed by computing the same three metrics as before, as well as the timescale at which the median is at 90% of its final value (the value at $t = 1000$ yr).

3. Results

3.1. Example Model Run

To illustrate individual simulations, Figure 4 shows two example runs, for sets of parameter values *Great South Bay* and *Core Sound* (found in Table 1). It shows how, in both cases, an initially undersaturated barrier coast with some storm-induced breaches (panel a & d) evolves under the influence of more storm-induced breaches (panel b & e) towards a ‘final’ configuration in which more inlets are open (panel c & f). During the simulation a number of storm-induced breaches remain open and evolve into tidal inlets while most eventually close. Our example simulation shows that not only do new breaches close, but in some cases if the new breach remains open, nearby prior inlets may close.

Furthermore, the example run for the *Great South Bay* (Figure 4 top row) shows an example of jump migration [38] where an inlet (the bottommost inlet) closes and a nearby breach remains open (effectively moving the inlet).

3.2. Monte Carlo Ensemble

To further analyze the impact of storm-induced breaches on barrier coast systems, we examine the results of two Monte Carlo ensembles for both the *Great South Bay* and *Core Sound* sets of parameter values (see Table 1).

Each Monte Carlo ensemble consists of 500 individual model runs, this number of individual model runs ensures that our results have converged, such that more runs would only change the result marginally. We find that even with the random forcing of breaches all three metrics (see Section 2.3.1) tend towards an equilibrium (see Figure 5). This means that the system reaches a dynamic equilibrium state, even with a continuous stochastic forcing of storm-induced breaches.

Comparison of the results for both sets of parameter values reveals that the equilibrium values and timescales are dependent on the set of parameter values. For all three metrics, the *Core Sound* system reaches its equilibrium values faster than the *Great South Bay* system. The former system approaches its equilibrium values very fast (the timescale in panel d & f coincides with the y -axis). The *Core Sound* system has less open inlets than the *Great South Bay* system (i.e., J_{total}/L is lower), while the inlets are larger (i.e., $A_{j,\text{all}}/A_{\mu}$ is larger).

The results for the Great South Bay also show that the dimensionless total tidal prism $P_{\text{total}}/P_{\text{ref,total}}$ approaches its dynamic equilibrium value first, followed by the ratio $A_{j,\text{all}}/A_{\mu}$, and finally the number of inlets J_{total}/L . Therefore, the configuration of the tidal inlets (i.e., size and spacing) takes longer to reach a dynamic equilibrium than the overall tidal prism of all inlets combined. This also explains why the ratio $A_{j,\text{all}}/A_{\mu}$ is initially relatively high; the dimensionless total tidal prism $P_{\text{total}}/P_{\text{ref,total}}$ increases faster than the number of open inlets per km barrier coast J_{total}/L , so each inlet conveys a larger part of the total tidal prism $P_{\text{total}}/P_{\text{ref,total}}$ than in the final state.

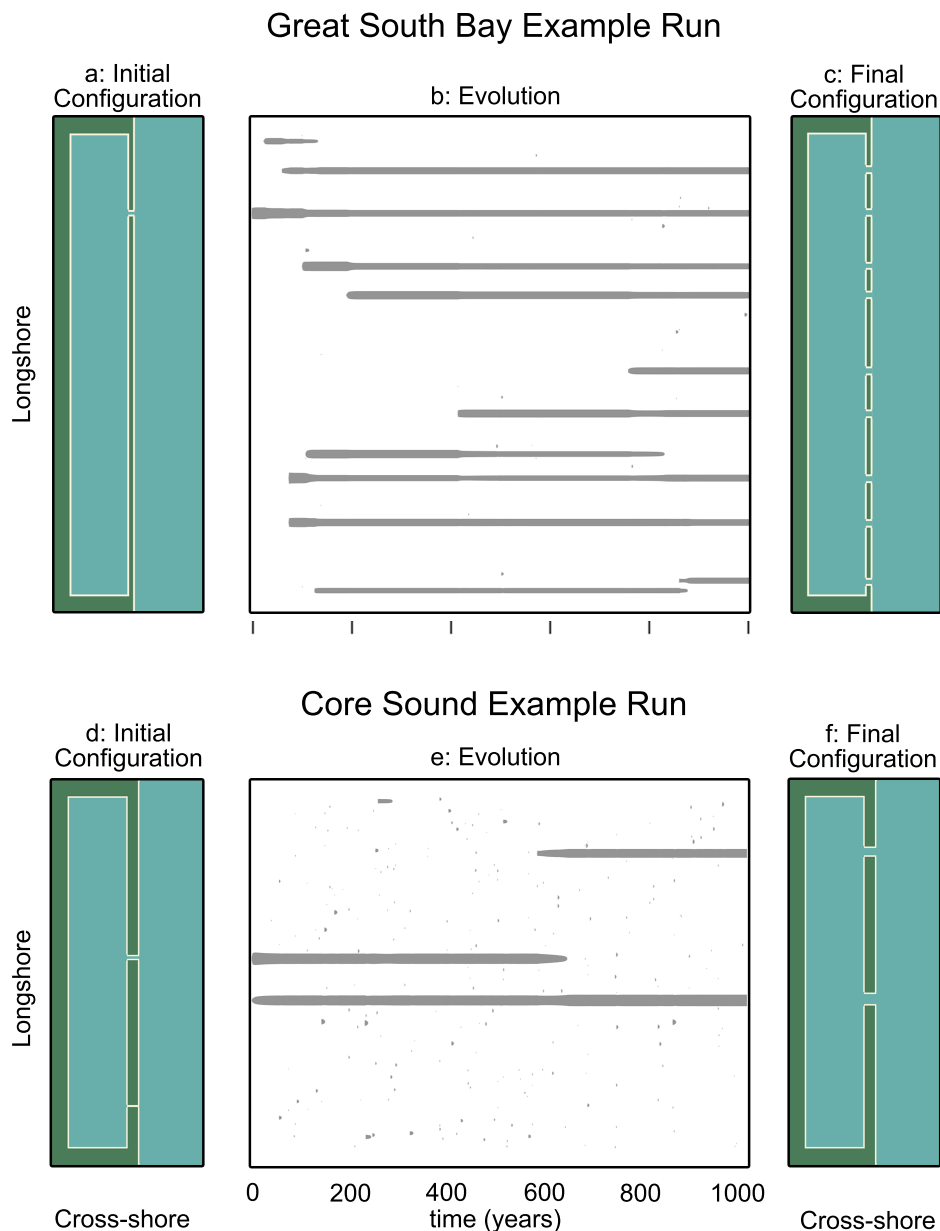


Figure 4. Two example runs for the sets of parameter values: Great South Bay (top), Core Sound (bottom). Shown are: the initial configuration with one open inlet (a,d); evolution of the system during which storm-induced breaches are stochastically forced (b,e); the final configuration with multiple open inlets (c,f). Please note that the grey dots correspond to breaches that quickly close after being randomly created.

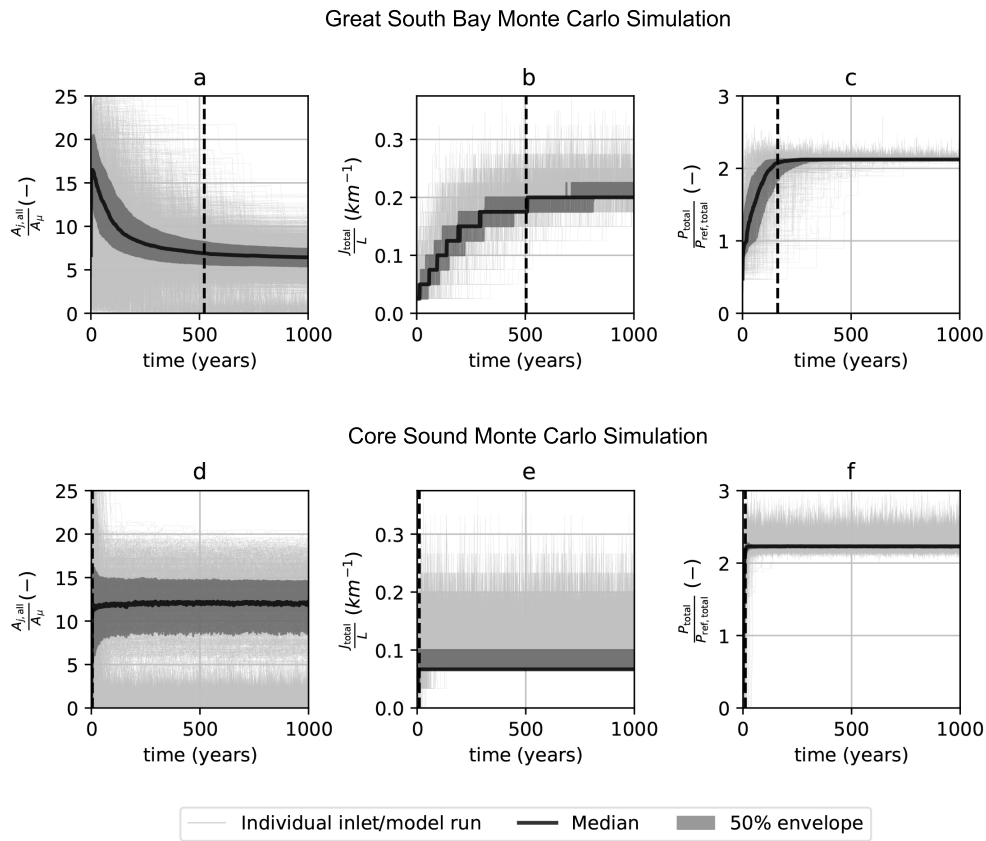


Figure 5. Results of two Monte Carlo simulations ($N = 500$) for both the Great South Bay (top) and Core Sound (bottom). Shown are: the ratio $A_{j,all}/A_{\mu}$ (a,d); the number of open inlets per km barrier coast J_{total}/L (b,e); dimensionless total tidal prism $P_{total}/P_{ref,total}$ (c,f), see Section 2.3. As these metrics are aggregated over all model runs, we show the mean (solid black), 50% envelope (dark grey), and individual model runs in light grey. The timescale to reach 90% of the final value has been indicated by dashed lines.

3.3. Breach Survival Chance

Next, we investigate how the three breach characteristics already introduced in Section 2.3.2, control the chance of a breach to survive and evolve into a stable tidal inlet. This is done by analyzing all storm-induced breaches that were forced in the Monte Carlo ensemble presented in the previous section. Figure 6 shows three histograms for all possible combinations of two breach characteristics.

These histograms show that the distance to the nearest neighbor $d_{nearest}$ is the breach characteristic that best predicts whether a breach will remain open or not. If a barrier coast is undersaturated (i.e., $J < 0.5J_{\mu}$), breaches closer to a nearest neighbor have an increased likelihood to remain open as well. Finally, the effect of the initial breach size A_{init} is that larger breaches slightly increase the chance of survival. This pattern was observed for both the Greath South Bay (left part Figure 6) and the Core Sound (right part Figure 6) sets of parameter values.

3.4. The Effects of Climate Change

The effect of changes in storm frequency due to climate change [37] is that the timescales for the system to reach its dynamic equilibrium change, but the resulting values in dynamic equilibrium do not change. This change in timescale (here defined as time required to reach $\pm 10\%$ of the final value at $t = 1000$ yr) is shown in Figure 7. The results show that an increase (decrease) in storm frequency clearly leads to a shorter (longer) timescale for all three metrics for the Great South Bay system. The timescale for the inlet cross-section $A_{j,all}/A_{\mu}$ and the number of open inlets per km

barrier coast J_{total}/L to reach their equilibrium value decreased from around 700 yr for $\lambda_s = 0.5$ to around 400 yr for $\lambda_s = 1.5$. For the total tidal prism $P_{\text{total}}/P_{\text{ref,total}}$ the timescale to reach its equilibrium decreased from over 300 yr for $\lambda_s = 0.5$ to just over 100 yr for $\lambda_s = 1.5$. For the Core Sound system, the timescale are very short already and barely changes due to variations in the storm frequency.

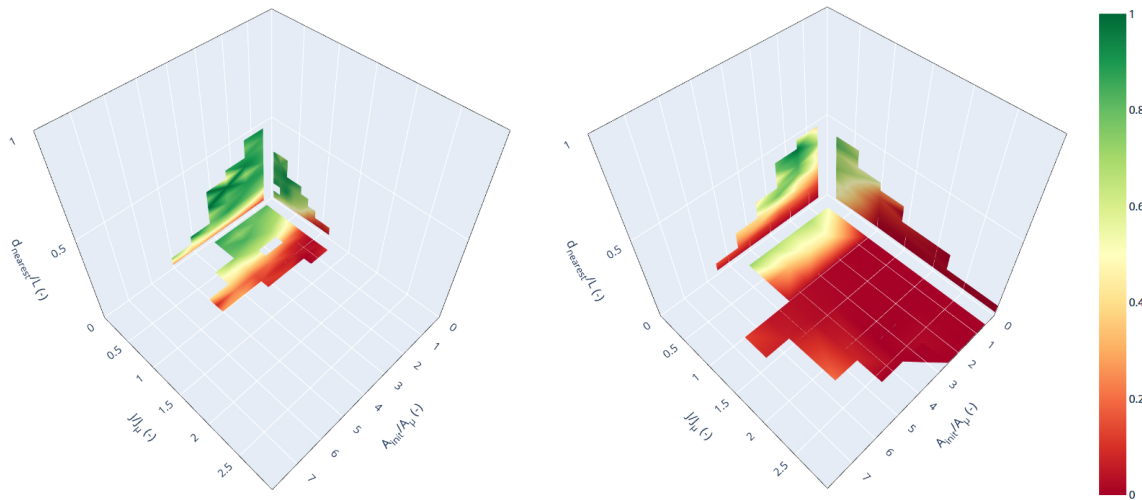


Figure 6. Breach survival chance shown for the simulations of Great South Bay (left) and Core Sound (right) sets of parameter values (see Table 1), in three histograms for varying values of relative initial breach size A_{init}/A_{μ} , barrier coast saturation J/J_{μ} , and distance to nearest neighboring inlet d_{nearest} .

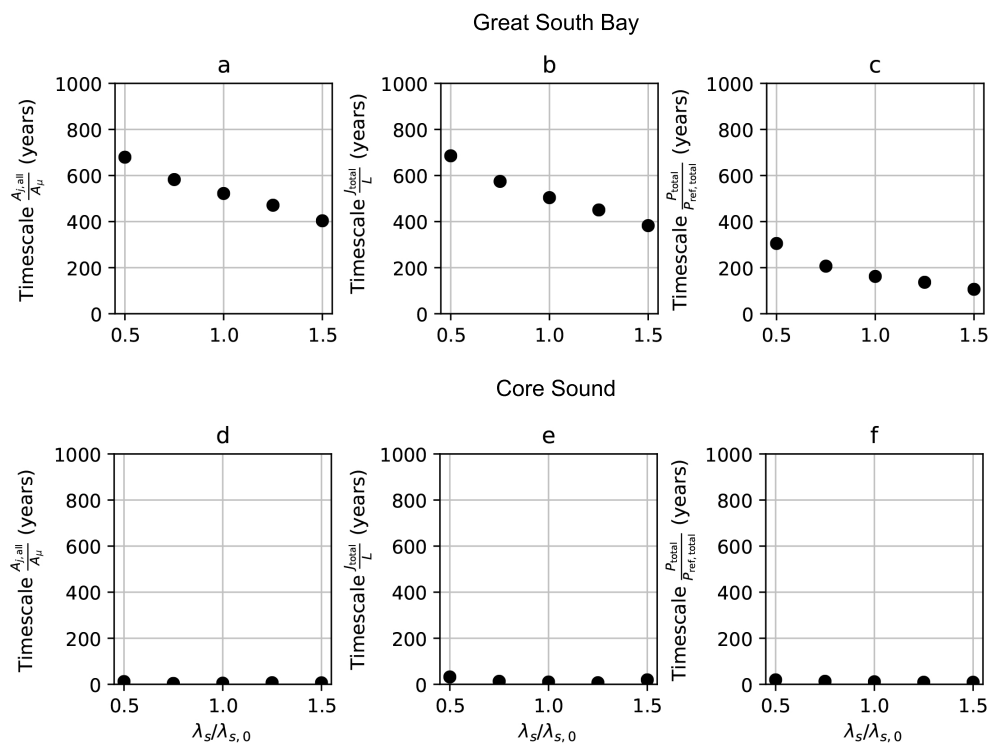


Figure 7. Effect of changes in storm frequency for the Great South Bay (top) and Core Sound (bottom) sets of parameter values (see Table 1). The timescales required to reach 90% of the final value of the same three metrics as in Figure 5 are plotted while storm frequency λ_s is changed between -50% and $+50\%$. Shown are the timescales for: the ratio $A_{j,\text{all}}/A_{\mu}$ (a,d); the number of open inlets per km barrier coast J_{total}/L (b,e); dimensionless total tidal prism $P_{\text{total}}/P_{\text{ref,total}}$ (c,f). N.B. the timescales for $\lambda_s/\lambda_{s,0} = 1.0$ corresponds to the dashed lines in Figure 5.

4. Discussion

4.1. System-Wide Equilibrium

Our results show how a barrier coast system will reach a dynamic equilibrium in terms of inlet cross-section $A_{j,\text{all}}/A_\mu$, the number of open inlets per km barrier coast J_{total}/L , and total tidal prism $P_{\text{total}}/P_{\text{ref,total}}$ while being stochastically forced by storm-induced breaches. Moreover, the systemwide equilibrium in total tidal prism $P_{\text{total}}/P_{\text{ref,total}}$ implies that if a breach remains open once this equilibrium has been reached, it will take over part of the tidal prism from the existing inlets, potentially leading to inlets closing. The above implies that a storm-induced breach that remains open affects barrier coast systems in two ways. First, a new breach directly provides a new connection between the outer sea and basin resulting in changed hydrodynamics in both. Second, that as a result a new breach indirectly affects the existing tidal inlets and the impact that they have on the hydrodynamics in both the outer sea and basin. Importantly, these two aspects are nonlinearly coupled.

Furthermore, we found that variations in storm frequency do not lead to a different total tidal prism, only the equilibrium timescale might change. This result implies that if the storm frequency increases, barrier coast systems will reach their dynamic equilibrium faster. So, if a barrier coast is moved away from its equilibrium state (e.g., due to human interventions such as closing newly opened breaches) more effort will be required to maintain the non-equilibrium state if the storm frequency increases. These findings agree with previous findings indicating that the total tidal prism for a barrier coast system is a system characteristic [13] and thus independent of storm frequency.

4.2. Survival of the Farthest

Our analysis on which breach characteristics are adequate predictors for the survival of a storm-induced breach showed that the distance to a neighboring inlet is the best predictor, followed by barrier coast saturation as second best and initial breach size as third.

The importance of a minimum distance between a new breach and a neighboring inlet indicates the need for a ‘barrier’ between different inlets for them both to remain stable. This finding is in agreement with previous findings of a minimum inlet spacing between multiple tidal inlets [12] and separations such as a topographic high (i.e., a tidal divide) leading to stable configurations for double inlet systems [39,40].

If a new breach close to an existing inlet drains the backbarrier basin more efficiently than the existing inlets, this could lead to the closure of the existing inlet. In this case, the new inlet succeeds in capturing part of the total tidal prism entering a backbarrier basin, which has been found to be a system characteristic [13]. Factors that were found to impact the minimum spacing of tidal inlets are the tidal range and backbarrier basin width [12,13]. Other factors that are likely to affect this minimum spacing are the depth of the basin h_b , length of an inlet l_j , and bottom friction in both the basin r_b and inlets r_j .

4.3. Model Validity & Limitations

In this work, we studied the impact of storm-induced breaches on barrier coast systems (i.e., not the actual breaching of barrier islands) and imitated the stochastic nature of storms in the idealized barrier coast model by Roos et al. [12]. Their earlier results showed a good qualitative agreement between the model results and observed relationships between inlet size and spacing and both tidal range and tidal basin width. Furthermore, Reef et al. [13] demonstrated that the model was capable of qualitatively reproducing the observed phenomena.

To assess the validity of how we stochastically simulate the storm capacity to induce breaches, we assess the results of the Monte Carlo ensemble. These results show that an equilibrium number of inlets is reached by the system, implying that most new breaches will close or cause a nearby inlet close. The example run (see Figure 4) also shows that most newly created breaches close as soon as the number of inlets has reached its equilibrium value. These results agree with observations from natural

systems in which numerous tidal inlets, that started as storm-induced breaches, have closed [17]. Examples of these natural systems are the barrier coasts systems considered in this study: the Great South Bay and the Core Sound system.

As a result of incorporating the most important processes that affect the long-term morphological evolution of barrier coast systems, our model is capable of capturing the most important qualitative behavior of the natural system. To attain a better quantitative description of the natural system, future work could include more morphological features that affect inlet locations such as tidal divides [39,40], washover deposits [15,16], relict inlet features [16], channel networks [41,42], and paleographic river valleys [43] that control inlet locations. Furthermore, additional processes can be considered such as basin and outer sea morphodynamics [41,44], changing boundary conditions due to climate change [1,2], and nonlinear hydrodynamics [8].

5. Conclusions

We studied the impact of storm-induced breaches on the long-term evolution of multiple-inlet systems to an equilibrium configuration. To do so, we performed a Monte Carlo simulation in which storm-induced breaches were stochastically forced using a newly created stochastic shell around an idealized barrier coast model. Using parameters representative for the Great South Bay and Core Sound, we determined that most breaches close while some remain open and develop towards a new stable inlet. The formation of a new inlet has a profound impact on the barrier coast system dynamics as a whole, as a new inlet (nonlinearly) affects not only the basin hydrodynamics, but also the morphodynamics of the neighboring inlets. Despite this, the system tends towards an equilibrium in terms of number of inlets and total tidal prism, while stochastically forced by storm-induced breaches.

By analyzing all storm-induced breaches in our Monte Carlo ensemble, we identified the distance to a neighboring inlet as the breach characteristic that is the best predictor for a breach to remain open or not. Finally, we also determined that an increase in storm frequency due to climate change can lead to a decrease of the timescale over which these equilibria are reached.

Author Contributions: Conceptualization, K.R.G.R. and P.C.R.; Data curation, K.R.G.R. and T.E.A.; Formal analysis, K.R.G.R. and T.E.A.; Funding acquisition, S.J.M.H.H.; Investigation, K.R.G.R. and T.E.A.; Methodology, K.R.G.R., P.C.R. and T.E.A.; Project administration, K.R.G.R., P.C.R. and S.J.M.H.H.; Resources, P.C.R. and S.J.M.H.H.; Software, K.R.G.R. and T.E.A.; Supervision, P.C.R., A.D. and S.J.M.H.H.; Validation, K.R.G.R.; Visualization, K.R.G.R. and T.E.A.; Writing—original draft, K.R.G.R.; Writing—review & editing, K.R.G.R., P.C.R., T.E.A., A.D. and S.J.M.H.H. All authors have read and agreed to the published version of the manuscript.

Funding: This research was carried out within the WADSnext! project, funded by the ‘Simon Stevin Meester’ prize (awarded by NWO to S.J.M.H.H.), Deltares, and the 4TU centre for Fluids and Solid Mechanics.

Acknowledgments: The authors wish to thank four graduate students who helped doing exploratory simulations. We also thank three anonymous reviewers for their helpful comments and J. Strickland for proofreading the manuscript.

Conflicts of Interest: The authors declare no conflict of interest. The funders had no role in the design of the study; in the collection, analyses, or interpretation of data; in the writing of the manuscript, or in the decision to publish the results.

References

1. Glaeser, J.D. Global Distribution of Barrier Islands in Terms of Tectonic Setting. *J. Geol.* **1978**, *86*, 283–297. [\[CrossRef\]](#)
2. Stutz, M.L.; Pilkey, O.H. Open-ocean barrier islands: Global influence of climatic, oceanographic, and depositional settings. *J. Coast. Res.* **2011**, *27*, 207–222. [\[CrossRef\]](#)
3. Oost, A.P.; Hoekstra, P.; Wiersma, A.; Flemming, B.; Lammerts, E.J.; Pejrup, M.; Hofstede, J.; van der Valk, B.; Kiden, P.; Bartholdy, J.; et al. Barrier island management: Lessons from the past and directions for the future. *Ocean. Coast. Manag.* **2012**, *68*, 18–38. [\[CrossRef\]](#)
4. Wang, Z.B.; Hoekstra, P.; Burchard, H.; Ridderinkhof, H.; De Swart, H.E.; Stive, M.J.F. Morphodynamics of the Wadden Sea and its barrier island system. *Ocean. Coast. Manag.* **2012**, *68*, 39–57. [\[CrossRef\]](#)

5. De Swart, H.E.; Zimmerman, J.T.F. Morphodynamics of Tidal Inlet Systems. *Annu. Rev. Fluid Mech.* **2009**, *41*, 203–229. [[CrossRef](#)]
6. Davis, R.A.; Hayes, M.O. What is a Wave-Dominated Coast? *Dev. Sedimentol.* **1984**, *39*, 313–329. [[CrossRef](#)]
7. Escoffier, E.F. The stability of tidal inlets. *Shore Beach* **1940**, *8*, 114–115.
8. Salles, P.; Voulgaris, G.; Aubrey, D.G. Contribution of nonlinear mechanisms in the persistence of multiple tidal inlet systems. *Estuarine Coast. Shelf Sci.* **2005**, *65*, 475–491. [[CrossRef](#)]
9. Duran-Matute, M.; Gerkema, T.; De Boer, G.J.; Nauw, J.J.; Gräwe, U. Residual circulation and freshwater transport in the Dutch Wadden Sea: A numerical modelling study. *Ocean. Sci.* **2014**, *10*, 611–632. [[CrossRef](#)]
10. Sassi, M.; Duran-Matute, M.; van Kessel, T.; Gerkema, T. Variability of residual fluxes of suspended sediment in a multiple tidal-inlet system: The Dutch Wadden Sea. *Ocean. Dyn.* **2015**, *65*, 1321–1333. [[CrossRef](#)]
11. Brouwer, R.L.; Schuttelaars, H.M.; Roos, P.C. Modelling the influence of spatially varying hydrodynamics on the cross-sectional stability of double inlet systems. *Ocean. Dyn.* **2013**, *63*, 1263–1278. [[CrossRef](#)]
12. Roos, P.C.; Schuttelaars, H.M.; Brouwer, R.L. Observations of barrier island length explained using an exploratory morphodynamic model. *Geophys. Res. Lett.* **2013**, *40*, 4338–4343. [[CrossRef](#)]
13. Reef, K.R.G.; Roos, P.C.; Schuttelaars, H.M.; Hulscher, S.J.M.H. Influence of backbarrier basin geometry on multiple tidal inlet systems: the roles of resonance and bottom friction. *J. Geophys. Res. Earth Surf.* **2020**. [[CrossRef](#)]
14. Sallenger, A.H. Storm Impact Scale for Barrier Islands. *J. Coast. Res.* **2000**, *16*, 890–895. [[CrossRef](#)]
15. Kraus, N.C.; Militello, A.; Todoroff, G. Barrier Beaching Processes and Barrier Spit Breach, Stone Lagoon, California. *Shore Beach* **2002**, *70*, 21–28.
16. Leatherman, S.P. Geomorphic and Stratigraphic Analysis of Fire Island, New York. *Mar. Geol.* **1985**, *63*, 173–195. [[CrossRef](#)]
17. Mallinson, D.J.; Smith, C.W.; Culver, S.J.; Riggs, S.R.; Ames, D. Geological characteristics and spatial distribution of paleo-inlet channels beneath the outer banks barrier islands, North Carolina, USA. *Estuarine Coast. Shelf Sci.* **2010**, *88*, 175–189. [[CrossRef](#)]
18. Vila-Concejo, A.; Matias, A.; Ferreira, Ó.; Duarte, C.; Dias, J. Recent Evolution of the Natural Inlets of a Barrier Island System in Southern Portugal. *J. Coast. Res.* **2002**, *36*, 741–752. [[CrossRef](#)]
19. Kombiadou, K.; Matias, A.; Ferreira, Ó.; Carrasco, A.R.; Costas, S.; Plomaritis, T. Impacts of human interventions on the evolution of the Ria Formosa barrier island system (S. Portugal). *Geomorphology* **2019**, *343*, 129–144. [[CrossRef](#)]
20. Hinrichs, C.; Flagg, C.N.; Wilson, R.E. Great South Bay After Sandy: Changes in Circulation and Flushing due to New Inlet. *Estuaries Coasts* **2018**, *41*, 2172–2190. [[CrossRef](#)]
21. Yu, J.; Wilson, R.E.; Flagg, C.N. A Hydraulic Model for Multiple-Bay-Inlet Systems on Barrier Islands. *Estuaries Coasts* **2018**, *41*, 373–383. [[CrossRef](#)]
22. FEMA. *Hurricane Sandy in New Jersey and New York (FEMA P-942)*; Technical Report November; FEMA: Washington, DC, USA, 2013.
23. Mallinson, J.; Culver, J.; Walsh, J.P.; Curtis, W. *Past, Present and Future Inlets of the outer Banks Barrier Islands, North Carolina*; Technical Report; East Carolina University: Greenville, NC, USA, 2008.
24. Van Goor, M.A.; Zitman, T.J.; Wang, Z.B.; Stive, M.J.F. Impact of sea-level rise on the morphological equilibrium state of tidal inlets. *Mar. Geol.* **2003**, *202*, 211–227. [[CrossRef](#)]
25. Dastgheib, A.; Roelvink, J.A.; Wang, Z.B. Long-term process-based morphological modeling of the Marsdiep Tidal Basin. *Mar. Geol.* **2008**, *256*, 90–100. [[CrossRef](#)]
26. Hosseini, S.R.; Marani, M.; Scaioni, M. *Statistical Distribution Fits for Hurricanes Parameters in the Atlantic Basin*; ASITA: Richmond, BC, USA, 2016; pp. 446–452.
27. Keim, B.D.; Muller, R.A.; Stone, G.W. Spatiotemporal patterns and return periods of tropical storm and hurricane strikes from Texas to Maine. *J. Clim.* **2007**, *20*, 3498–3509. [[CrossRef](#)]
28. Google. *Map data: SIO, NOAA, U.S. Navy, NGA, GEBCO, TerraMetrics*; Google: Menlo Park, CA, USA.
29. Vogel, M.J.; Kana, T.W. *Sedimentation Patterns in a Tidal Inlet System Moriches Inlet, New York*; Coastal Engineering Proceedings; ASCE: Reston, VA, USA, 1984; pp. 3017–3033. [[CrossRef](#)]
30. MacIvor, L.H.; Motivans, K. *Impacts to Piping Plover and Seabeach Amaranth from Long-Term Sand Management Component*; Technical Report; US Army Corps of Engineers, Baltimore, MD, USA 1998.
31. Matias, A.; Ferreira, Ó.; Alveirinho-Dias, J.M. Preliminary results of the Cacela Peninsula (southern Portugal) replenishment. *Bol. Inst. Esp. Oceanogr* **1999**, *15*, 283–288.

32. Cañizares, R.; Irish, J.L. Simulation of storm-induced barrier island morphodynamics and flooding. *Coast. Eng.* **2008**, *55*, 1089–1101. [[CrossRef](#)]
33. Wamsley, T.V.; Hathaway, K.K.; Wutkowski, M. *Hatteras Breach, North Carolina*; Technical Report; US Army Corps of Engineers: Washington, DC, USA, 2010.
34. Clinch, A.S.; Russ, E.R.; Oliver, R.C.; Mitsova, H.; Overton, M.F. Hurricane Irene and the Pea Island breach: prestorm site characterization and storm surge estimation using geospatial technologies. *Shore Beach* **2012**, *80*, 38–46.
35. Flagg, C.; Hinrichs, C.; Flood, R.; Wilson, R. *Update on the Status of Old Inlet Breach*; Stony Brook University, School of Marine and Atmospheric Science, NY, USA 2016.
36. Safak, I.; Warner, J.C.; List, J.H. Barrier island breach evolution: Alongshore transport and bay-ocean pressure gradient interactions. *J. Geophys. Res. Ocean.* **2016**, *121*, 8720–8730. [[CrossRef](#)]
37. Christensen, J.; Kumar, K.K.; Aldria, E.; An, S.I.; Cavalcanti, I.; Castro, M.D.; Dong, W.; Goswami, P.; Hall, A.; Kanyanga, J.; et al. Climate Phenomena and their Relevance for Future Regional Climate Change Supplementary Material. *arXiv* **2013**, arXiv:1011.1669v3. doi:10.1017/CBO9781107415324.028.
38. Vila-Concejo, A.; Matias, A.; Pacheco, A.; Ferreira, Ó.; Dias, J.A. Quantification of inlet-related hazards in barrier island systems. An example from the Ria Formosa (Portugal). *Cont. Shelf Res.* **2006**, *26*, 1045–1060. [[CrossRef](#)]
39. Van de Kreeke, J.; Brouwer, R.L.; Zitman, T.J.; Schuttelaars, H.M. The effect of a topographic high on the morphological stability of a two-inlet bay system. *Coast. Eng.* **2008**, *55*, 319–332. [[CrossRef](#)]
40. De Swart, H.E.; Volp, N.D. Effects of hypsometry on the morphodynamic stability of single and multiple tidal inlet systems. *J. Sea Res.* **2012**, *74*, 35–44. [[CrossRef](#)]
41. Kragtwijk, N.G.; Zitman, T.J.; Stive, M.J.F.; Wang, Z.B. Morphological response of tidal basins to human interventions. *Coast. Eng.* **2004**, *51*, 207–221. [[CrossRef](#)]
42. Reef, K.R.G.; Lipari, G.; Roos, P.C.; Hulscher, S.J.M.H. Time-varying storm surges on Lorentz's Wadden Sea networks. *Ocean. Dyn.* **2018**, *68*, 1051–1065. [[CrossRef](#)]
43. FitzGerald, D.M. Geomorphic Variability and Morphologic and Sedimentologic Controls on Tidal Inlets. *J. Coast. Res.* **1996**, 47–71. [[CrossRef](#)]
44. Elias, E.P.L.; Van Der Spek, A.J.; Wang, Z.B.; De Ronde, J. Morphodynamic development and sediment budget of the Dutch Wadden Sea over the last century. *Geol. Mijnbouw/Netherlands J. Geosci.* **2012**, *91*, 293–310. [[CrossRef](#)]



© 2020 by the authors. Licensee MDPI, Basel, Switzerland. This article is an open access article distributed under the terms and conditions of the Creative Commons Attribution (CC BY) license (<http://creativecommons.org/licenses/by/4.0/>).